Inorg. Chem. **2008**, *47*, 2786−2797

Comparing Main Group and Transition-Metal Square-Planar Complexes of the Diselenoimidodiphosphinate Anion: A Solid-State NMR Investigation of $M[N(^iPr_2PSe)_2]_2$ (M = Se, Te; Pd, Pt)

Bryan A. Demko and Roderick E. Wasylishen*

Department of Chemistry, Gunning/Lemieux Chemistry Centre, University of Alberta, Edmonton, AB T6G 2G2, Canada

Received October 9, 2007

A comparison of the square-planar complexes of group 10 (Pd^{II}, Pt^{II}) and 16 (Se^{II}, Te^{II}) centers with the tetraisopropyldiselenoimidodiphosphinate anion, $[N(^iPr_2PSe)_2]^-$, is made on the basis of the results of a solid-state ^{31}P, ^{77}Se, ^{125}Te, and ^{195}Pt NMR investigation. Density functional theory calculations of the respective chemical shift and ^{14}N electric field gradient tensors in these compounds complement the experimental results. The NMR spectra were analyzed to determine the respective phosphorus, selenium, tellurium, and platinum chemical shift tensors along with numerous indirect spin–spin coupling constants. Special attention was given to observed differences in the NMR parameters for the transition metal and main-group square-planar complexes. Residual dipolar coupling between ^{14}N and ^{31}P, not observed in the solid-state ^{31}P NMR spectra of the Pd(II) and Pt(II) complexes, was observed at 4.7 and 7.0 T for $M[N(^iPr_2PSe)_2]_2$ (M = Se, Te) yielding average values of $R(^{31}P,^{14}N)_{eff}$ = 890 Hz, $C_Q(^{14}N)$ = 2.5 MHz, $^1J(^{31}P,^{14}N)_{iso}$= 15 Hz, $\alpha = 90°$, $\beta = 17°$. The span, Ω, and calculated orientation of the selenium chemical shift tensor for the diselenoimidodiphosphinate anion is found to depend on whether the selenium is located within a pseudoboat or distorted-chair MSe_2P_2N six-membered ring. The largest reported values of $^1J(^{77}Se,^{77}Se)_{iso}$, 405 and 435 Hz, and $^1J(^{125}Te,^{77}Se)_{iso}$, 1120 and 1270 Hz, were obtained for the selenium and tellurium complexes, respectively; however, in contrast a correspondingly large value of $^1J(^{195}Pt,^{77}Se)_{iso}$ was not found. The chemical shift tensors for the central atoms, Se(II) and Te(II), possess positive skews, while for Pt(II) its chemical shift tensor has a negative κ. This observed difference for the shielding of the central atoms has been explained using a qualitative molecular orbital approach.

Introduction

The diselenoimidodiphosphinate anion, $[N(R_2PSe)_2]^-$ (R = alkyl, aryl), a bidentate ligand often referred to as the inorganic analogue of acetyl acetonate, has been utilized in the preparation of homoleptic square-planar complexes of both main-group[1–5] and transition-metal[6–8] centers. Dichalcogenoimidodiphosphinato complexes, $M^{n+}[N(R_2PE)_2]_n$ (E = O, S, Se, Te), are known to exhibit various binding geometries about the metal center that depend on the choice of chalcogen, organic group, and complexing metal.[9–13] The flexibility of the dichalcogenoimidodiphosphinate system has been called one of its greatest advantages, permitting the

* Corresponding author. Phone: 780 492-4336.Fax: 780 492-8231. E-mail: roderick.wasylishen@ualberta.ca.

(1) Cea-Olivares, R.; Canseco-Melchor, G.; García-Montalvo, V.; Hernández-Ortega, S.; Novosad, J. *Eur. J. Inorg. Chem.* **1998**, 1573–1576.
(2) Cea-Olivares, R.; Novosad, J.; Woollins, J. D.; Slawin, A. M. Z.; García-Montalvo, V.; Espinosa-Pérez, G.; García y García, P. *Chem. Commun.* **1996**, 519–520.
(3) Cea-Olivares, R.; Moya-Cabrera, M.; García-Montalvo, V.; Castro-Blanco, R.; Toscano, R. A.; Hernández-Ortega, S. *Dalton Trans.* **2005**, 1017–1018.
(4) Birdsall, D. J.; Novosad, J.; Slawin, A. M. Z.; Woollins, J. D. *Dalton Trans.* **2000**, 435–439.
(5) Novosad, J.; Lindeman, S. V.; Marek, J.; Woollins, J. D.; Husebye, S. *Heteroatom Chem.* **1998**, *9*, 615–621.
(6) Bhattacharyya, P.; Novosad, J.; Phillips, J.; Slawin, A. M. Z.; Williams, D. J.; Woollins, J. D. *Dalton Trans.* **1995**, 1607–1613.
(7) Papadimitriou, C.; Veltsistas, P.; Novosad, J.; Cea-Olivares, R.; Toscano, A.; García y García, P.; Lopez-Cardosa, M.; Slawin, A. M. Z.; Woollins, J. D. *Polyhedron* **1997**, *16*, 2727–2729.
(8) Cupertino, D.; Birdsall, D. J.; Slawin, A. M. Z.; Woollins, J. D. *Inorg. Chim. Acta* **1999**, *290*, 1–7.
(9) Haiduc, I.; Silaghi-Dumitrescu, I. *Coord. Chem. Rev.* **1986**, *74*, 127–270.
(10) Woollins, J. D. *Dalton Trans.* **1996**, 2893–2901.
(11) Silvestru, C.; Drake, J. E. *Coord. Chem. Rev.* **2001**, *223*, 117–216.
(12) Ly, T. Q.; Woollins, J. D. *Coord. Chem. Rev.* **1998**, *176*, 451–481.
(13) Bhattacharyya, P.; Woollins, J. D. *Polyhedron* **1995**, *14*, 3367–3388.

10.1021/ic7019999 CCC: $40.75
Published on Web 02/13/2008

EPNPE skeleton to adjust to various coordination geometries desired by the central metal,[11,14] along with the large chalcogen−chalcogen "bite", which aids in forming regular coordination spheres with large central atoms.[15] These bidentate ligands have found applications as single-source precursors for solid-state metal chalcogenide materials,[16–34] in the search for stereochemically active lone pairs,[2,3,6,8,35–46] in catalysis,[47–49] and in metal extraction processes,[13,43,50–57] as lanthanide shift reagents,[43,58–62] as luminescent materials,[63] and as enzyme mimetics.[64–66]

Considerable interest persists for square-planar complexes, yet appropriate comparisons between main-group and transition-metal centers are difficult, as few analogous systems exist. The homoleptic group 10 and 16 tetraisopropyldiselenoimidodiphosphinato complexes, $M[N(^iPr_2PSe)_2]_2$ (M = Pd, Pt and Se, Te, respectively), offer a rare opportunity to probe the differences between main-group and traditional transition-metal square-planar systems. Solid-state NMR is aptly suited for investigating the detailed molecular environments of the diselenoimidodiphosphinato complexes, and we have recently demonstrated the utility of solid-state NMR spectroscopy in the characterization of the group 12 metal complexes of the $[N(^iPr_2PSe)_2]^-$ ligand.[67] In the present study, a combined density functional theory, DFT, and experimental solid-state ^{31}P, ^{77}Se, ^{125}Te, and ^{195}Pt NMR investigation of the square-planar $M[N(^iPr_2PSe)_2]_2$ (M = Pd, Pt; Se, Te) complexes is reported.

Experimental Section

Preparation of Complexes. Iminobis(diisopropylphosphine selenide), $HN(^iPr_2PSe)_2$, was prepared according to the two-step condensation followed by oxidation procedure outlined in the

(14) Balazs, L.; Stanga, O.; Breunig, H. J.; Silvestru, C. *Dalton Trans.* **2003**, 2237–2242.
(15) Darwin, K.; Gilby, L. M.; Hodge, P. R.; Piggott, B. *Polyhedron* **1999**, *18*, 3729–3733.
(16) Afzaal, M.; Crouch, D.; Malik, M. A.; Motevalli, M.; O'Brien, P.; Park, J.-H. *J. Mater. Chem.* **2003**, *13*, 639–640.
(17) Afzaal, M.; Crouch, D. J.; O'Brien, P.; Raftery, J.; Skabara, P. J.; White, A. J. P.; Williams, D. J. *J. Mater. Chem.* **2004**, *14*, 233–237.
(18) Crouch, D. J.; Helliwell, M.; O'Brien, P.; Park, J.-H.; Waters, J.; Williams, D. J. *Dalton Trans.* **2003**, 1500–1504.
(19) Pickett, N. L.; O'Brien, P. *Chem. Rec.* **2001**, *1*, 467–479.
(20) Green, M.; O'Brien, P. *Chem. Commun.* **1999**, 2235–2241.
(21) Gleizes, A. N. *Chem. Vap. Deposition* **2000**, *6*, 155–173.
(22) Afzaal, M.; Aucott, S. M.; Crouch, D.; O'Brien, P.; Woollins, J. D.; Park, J.-H. *Chem. Vap. Deposition* **2002**, *8*, 187–189.
(23) Afzaal, M.; Crouch, D.; Malik, M. A.; Motevalli, M.; O'Brien, P.; Park, J.-H.; Woollins, J. D. *Eur. J. Inorg. Chem.* **2004**, 171–177.
(24) Malik, M. A.; Afzaal, M.; O'Brien, P.; Halliwell, M. *Polyhedron* **2006**, *25*, 864–868.
(25) Afzaal, M.; Ellwood, K.; Pickett, N. L.; O'Brien, P.; Raftery, J.; Waters, J. *J. Mater. Chem.* **2004**, *14*, 1310–1315.
(26) Park, J.-H.; Afzaal, M.; Helliwell, M.; Malik, M. A.; O'Brien, P.; Raftery, J. *Chem. Mater.* **2003**, *15*, 4205–4210.
(27) Waters, J.; Crouch, D.; O'Brien, P.; Park, J.-H. *J. Mater. Sci.: Mater. Electron.* **2003**, *14*, 599–602.
(28) Waters, J.; Crouch, D.; Raftery, J.; O'Brien, P. *Chem. Mater.* **2004**, *16*, 3289–3298.
(29) Crouch, D. J.; O'Brien, P.; Malik, M. A.; Skabara, P. J.; Wright, S. P. *Chem. Commun.* **2003**, 1454–1455.
(30) Singhal, A.; Dutta, D. P.; Kulshreshtha, S. K.; Mobin, S. M.; Mathur, P. *J. Organomet. Chem.* **2006**, *691*, 4320–4328.
(31) Garje, S. S.; Copsey, M. C.; Afzaal, M.; O'Brien, P.; Chivers, T. *J. Mater. Chem.* **2006**, *16*, 4542–4547.
(32) Garje, S. S.; Ritch, J. S.; Eisler, D. J.; Afzaal, M.; O'Brien, P.; Chivers, T. *J. Mater. Chem.* **2006**, *16*, 966–969.
(33) Copsey, M. C.; Panneerselvam, A.; Afzaal, M.; Chivers, T.; O'Brien, P. *Dalton Trans.* **2007**, 1528–1538.
(34) Ritch, J. S.; Chivers, T.; Afzaal, M.; O'Brien, P. *Chem. Soc. Rev.* **2007**, *36*, 1622–1631.
(35) Rossi, R.; Marchi, A.; Marvelli, L.; Magon, L.; Peruzzini, M.; Casellato, U.; Graziani, R. *Dalton Trans.* **1993**, 723–729.
(36) Cea-Olivares, R.; García-Montalvo, V.; Novosad, J.; Kilian, P.; Woollins, J. D.; Slawin, A. M. Z.; García y García, P.; López-Cardoso, M.; Espinosa-Pérez, G.; Toscano, R. A.; Hernández, S.; Canseco-Melchor, G.; Lima-Montaño, L.; Rodríguez-Narváez, C. *Phosphorus Sulfur Silicon Relat. Elem.* **1997**, *124*, 347–354.
(37) Chivers, T.; Konu, J.; Ritch, J. S.; Copsey, M. C.; Eisler, D. J.; Tuononen, H. M. *J. Organomet. Chem.* **2007**, *692*, 2658–2668.
(38) Cupertino, D.; Keyte, R.; Slawin, A. M. Z.; Williams, D. J.; Woollins, J. D. *Inorg. Chem.* **1996**, *35*, 2695–2697.
(39) Williams, D. J.; Quicksall, C. O.; Barkigia, K. M. *Inorg. Chem.* **1982**, *21*, 2097–2100.
(40) Cea-Olivares, R.; Toscano, R. A.; Carreón, G.; Valdés-Martínez, J. *Monatsh. Chem.* **1992**, *123*, 391–396.
(41) García-Montalvo, V.; Novosad, J.; Kilian, P.; Woollins, J. D.; Slawin, A. M. Z.; García y García, P.; López-Cardoso, M.; Espinosa-Pérez, G.; Cea-Olivares, R. *Dalton Trans.* **1997**, 1025–1029.
(42) García-Montalvo, V.; Zamora-Rosete, M. K.; Gorostieta, D.; Cea-Olivares, R.; Toscano, R. A.; Hernández-Ortega, S. *Eur. J. Inorg. Chem.* **2001**, 2279–2285.
(43) Rodríguez, I.; Alvarez, C.; Gómez-Lara, J.; Cea-Olivares, R. *Lanthanide Actinide Res.* **1986**, *1*, 253–260.
(44) Silvestru, C.; Haiduc, I.; Cea-Olivares, R.; Zimbron, A. *Polyhedron* **1994**, *13*, 3159–3165.
(45) Cea-Olivares, R.; García-Montalvo, V.; Novosad, J.; Woollins, J. D.; Toscano, R. A.; Espinosa-Pérez, G. *Chem. Ber.* **1996**, *129*, 919–923.
(46) García-Montalvo, V.; Cea-Olivares, R.; Williams, D. J.; Espinosa-Pérez, G. *Inorg. Chem.* **1996**, *35*, 3948–3953.
(47) Rudler, H.; Denise, B.; Gregorio, J. R.; Vaissermann, J. *Chem. Commun.* **1997**, 2299–2300.
(48) Goyal, M.; Novosad, J.; Necas, M.; Ishii, H.; Nagahata, R.; Sugiyama, J.-I.; Asai, M.; Ueda, M.; Takeuchi, K. *Appl. Organomet. Chem.* **2000**, *14*, 629–633.
(49) Chatziapostolou, K. A.; Vallianatou, K. A.; Grigoropoulos, A.; Raptopoulou, C. P.; Terzis, A.; Kostas, I. D.; Kyritsis, P.; Pneumatikakis, G. *J. Organomet. Chem.* **2007**, *692*, 4129–4138.
(50) du Preez, J. G. H.; Knabl, K. U.; Krüger, L.; van Brecht, B. J. A. M. *Solvent Extr. Ion Exch.* **1992**, *10*, 729–748.
(51) Navrátil, O.; Herrmann, E.; Grossmann, G.; Teplý, J. *Collect. Czech. Chem. Commun.* **1990**, *55*, 364–371.
(52) Herrmann, E.; Navrátil, O.; Nang, H. b.; Smola, J.; Friedrich, J.; Príhoda, J.; Dreyer, R.; Chalkin, V. A.; Kulpe, S. *Collect. Czech. Chem. Commun.* **1984**, *49*, 201–217.
(53) Navrátil, O.; Cigánek, M.; Herrmann, E. *Collect. Czech. Chem. Commun.* **1983**, *48*, 2009–2014.
(54) Navrátil, O.; Fofana, M.; Smola, J. *Z. Chem.* **1984**, 24–30.
(55) Navrátil, O.; Herrmann, E.; Slezák, P. *Collect. Czech. Chem. Commun.* **1987**, *52*, 1708–1714.
(56) Muñoz-Hernández, M.-Á.; Singer, A.; Atwood, D. A.; Cea-Olivares, R. *J. Organomet. Chem.* **1998**, *571*, 15–19.
(57) Le, Q. T. H.; Umetani, S.; Matsui, M. *Dalton Trans.* **1997**, 3835–3840.
(58) Platzer, N.; Rudler, H.; Alvarez, C.; Barkaoui, L.; Denise, B.; Goasdoué, N.; Rager, M.-N.; Vaissermann, J.; Daran, J.-C. *Bull. Soc. Chim. Fr.* **1995**, *132*, 95–113.
(59) Alvarez, C.; Barkaoui, L.; Goasdoué, N.; Daran, J.-C.; Platzer, N.; Rudler, H.; Vaissermann, J. *Chem. Commun.* **1989**, 1507–1509.
(60) Alvarez, C.; Goasdoué, N.; Platzer, N.; Rodríguez, I.; Rudler, H. *Chem. Commun.* **1988**, 1002–1004.
(61) Barkaoui, L.; Charrouf, M.; Rager, M.-N.; Denise, B.; Platzer, N.; Rudler, H. *Bull. Soc. Chim. Fr.* **1997**, *134*, 167–175.
(62) Rodríguez, I.; Alvarez, C.; Gómez-Lara, J.; Toscano, R. A.; Platzer, N.; Mulheim, C.; Rudler, H. *Chem. Commun.* **1987**, 1502–1503.
(63) Magennis, S. W.; Parsons, S.; Corval, A.; Woollins, J. D.; Pikramenou, Z. *Chem. Commun.* **1999**, 61–62.
(64) Bereman, R. D.; Wang, F. T.; Najdzionek, J.; Braitsch, D. M. *J. Am. Chem. Soc.* **1976**, *98*, 7266–7268.
(65) Sakaguchi, U.; Addison, A. W. *J. Am. Chem. Soc.* **1977**, *99*, 5189–5190.
(66) Siiman, O.; Vetuskey, J. *Inorg. Chem.* **1980**, *19*, 1672–1680.
(67) Demko, B. A.; Wasylishen, R. E. *Dalton Trans.* **2008**, 481–490.

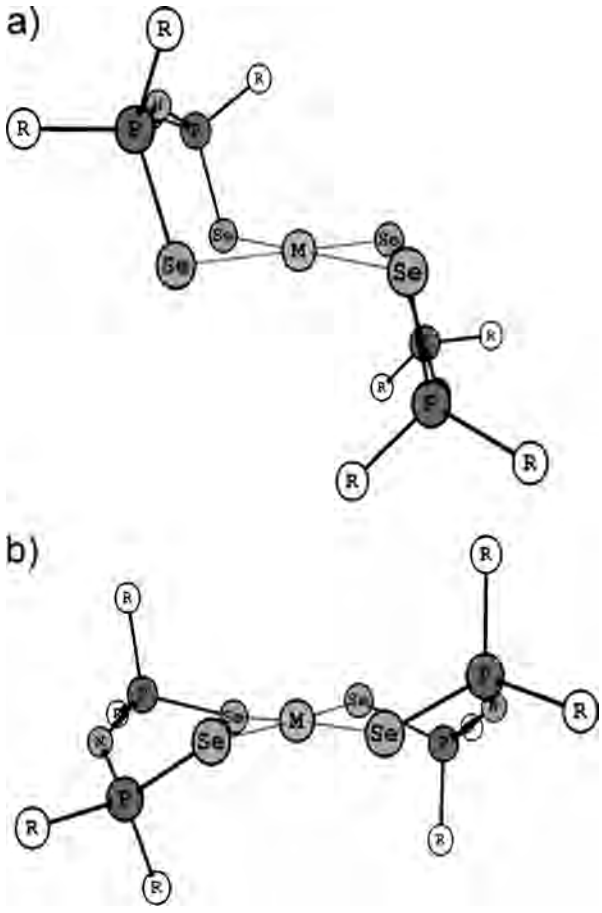

Figure 1. Representation of the solid-state structures of $M[N(R_2PSe)_2]_2$ (R = ^{i}Pr, Ph) (a) M = Se, Te; (b) M = Pd, Pt.

literature.[68] The transition-metal complexes were obtained by slow addition of the corresponding dichloro(1,5-cyclooctadiene)metal(II) into a basic methanol solution of tetraisopropyldiselenoimidodiphosphinate, $[N(^iPr_2PSe)_2]^-$, as described by Cupertino et al.[8] The main-group complexes were prepared in a similar fashion from $[N(^iPr_2PSe)_2]^-$ with $Se[S_2P(O^iPr)_2]_2$ and $Te(thiourea)_4Cl_2 \cdot 2H_2O$, respectively, according to literature procedures.[3,4] Crystal structures have previously been determined for the square-planar complexes, $M[N(^iPr_2PSe)_2]_2$ (M = Pt,[8] Se,[3] Te[4]), and a representation of their structures is given in Figure 1. All structures indicate a single $M[N(^iPr_2PSe)_2]_2$ molecule in the asymmetric unit; however, the main-group centered structures (Figure 1a) crystallize within the $P2_1/c$ space group, while the transition-metal structure (Figure 1b) crystallizes in the $C2/c$ space group.

NMR Experiments. Solution ^{77}Se and ^{195}Pt NMR spectra for a $CDCl_3$ solution of $Pt[N(^iPr_2PSe)_2]_2$ were acquired, at 76.3 and 85.6 MHz, respectively, on a 9.4 T spectrometer in order to deduce the magnitudes of the platinum−selenium and platinum−phosphorus indirect spin–spin coupling constants.

Solid-state NMR investigations of powdered samples of $M[N(^iPr_2PSe)_2]_2$ (M = Pd, Pt; Se, Te) were obtained on 4.7, 7.0, and 11.7 T NMR spectrometers. The samples were packed in 4 mm (7.0 and 11.7 T) and 7.5 mm (4.7 T) o.d. zirconium oxide rotors and were placed within probes suitable for magic angle spinning, MAS, NMR experiments. A variable amplitude cross-polarization, VACP, pulse sequence was used to acquire all spectra.[69] Proton-decoupling fields of approximately 60 kHz were achieved via two-pulse phase modulation, TPPM.[70] The ^{31}P NMR spectra were referenced with respect to 85% H_3PO_4 (aq) by setting the isotropic ^{31}P NMR peak of solid $(NH_4)H_2PO_4$ to 0.81 ppm.[71] Similarly, ^{77}Se NMR spectra were referenced to Me_2Se (l) by setting the isotropic peak of solid ammonium selenate to 1040.2 ppm.[71,72] Tellurium-125 NMR spectra were referenced with respect to dimethyl telluride by setting the high frequency solid-state ^{125}Te NMR peak of telluric acid to 692.2 ppm.[71,73] Solid-state ^{195}Pt NMR spectra were referenced to potassium hexachloroplatinate by setting the ^{195}Pt NMR peak of solid $K_2Pt(OH)_6$ to 3476 ppm.[71,74]

Solid-state ^{31}P NMR experiments were performed at Larmor frequencies of 81.0, 121.6, and 202.5 MHz and at spinning frequencies ranging from 1.50 to 5.00 kHz. A total of between 32 and 512 scans were acquired per spectrum. Contact times between 1.5 and 6.5 ms and pulse delays between 5 and 20 s were employed.

Solid-state ^{77}Se NMR measurements were performed at Larmor frequencies of 38.2, 57.3, and 95.4 MHz and at spinning frequencies ranging from 2.35 to 12.00 kHz. A total of between 880 and 31808 scans were acquired per spectrum. Contact times between 7.0 and 10.0 ms and pulse delays between 5 and 11 s were employed.

Solid-state ^{125}Te NMR experiments on $Te[N(^iPr_2PSe)_2]_2$ were performed at Larmor frequencies of 63.2 and 94.8 MHz, and at spinning frequencies ranging from 5.00 to 12.00 kHz. A total of between 25616 and 41520 scans were acquired per spectrum. Contact times between 8.0 and 11.0 ms and pulse delays between 8 and 20 s were employed.

Solid-state ^{195}Pt NMR experiments on $Pt[N(^iPr_2PSe)_2]_2$ were performed at 42.8 MHz at spinning speeds ranging from 6.00 to 6.75 kHz. A total of between 19904 and 84656 scans were acquired per spectrum. Contact times and pulse delays of 11.0 ms and 9 s were employed, respectively.

The principal components of the respective phosphorus, selenium, tellurium, and platinum chemical shift tensors, $\delta_{11} \geq \delta_{22} \geq \delta_{33}$, were determined from the experimental spectra via the procedure of Herzfeld and Berger.[75,76] All experimental solid-state NMR spectra were simulated using the determined values with the program WSOLIDS[77] to assess the quality of the obtained parameters. This procedure results in errors of ±0.2 ppm in the isotropic chemical shift, $\delta_{iso} = (1/3)(\delta_{11} + \delta_{22} + \delta_{33})$, and errors in the principal components about 1–3% of the span, $\Omega = \delta_{11} - \delta_{33}$, of the respective chemical shift tensor. Another useful quantity for describing the appearance of chemical shift tensors is the skew, $\kappa = 3(\delta_{22} - \delta_{iso})/\Omega$.[78]

DFT Computations. Theoretical calculation of NMR parameters, particularly for heavier nuclei where interpretations are more difficult than those extracted from ^{13}C NMR spectra, has become increasingly useful for spectroscopists.[79] Magnetic shielding tensors,

(68) Haiduc, I. In *Inorganic Experiments*; Woollins, J. D., Ed.; VCH: New York, Basel, Cambridge, Tokyo, 1994; pp 145–149..

(69) Metz, G.; Wu, X.; Smith, S. O. *J. Magn. Reson. Ser. A* **1994**, *110*, 219–227.
(70) Bennett, A. E.; Rienstra, C. M.; Auger, M.; Lakshmi, K. V.; Griffin, R. G. *J. Chem. Phys.* **1995**, *103*, 6951–6958.
(71) Bryce, D. L.; Bernard, G. M.; Gee, M.; Lumsden, M.; Eichele, K.; Wasylishen, R. E. *Can. J. Anal. Sci. Spectrosc.* **2001**, *46*, 46–82.
(72) Collins, M. J.; Ratcliffe, C. I.; Ripmeester, J. A. *J. Magn. Reson.* **1986**, *68*, 172–179.
(73) Collins, M. J.; Ripmeester, J. A. *J. Am. Chem. Soc.* **1987**, *109*, 4113–4115.
(74) Harris, R. K.; Sebald, A. *Magn. Reson. Chem.* **1987**, *25*, 1058–1062.
(75) Maricq, M. M.; Waugh, J. S. *J. Chem. Phys.* **1979**, *70*, 3300–3316.
(76) Herzfeld, J.; Berger, A. E. *J. Chem. Phys.* **1980**, *73*, 6021–6030.
(77) Eichele, K.; Wasylishen, R. E. 1.17.30 ed., 2001.
(78) Mason, J. *Solid State Nucl. Magn. Reson.* **1993**, *2*, 285–288.
(79) Pulay, P. In *Calculation of NMR and EPR Parameters*; Kaupp, M., Bühl, M., Malkin, V. G., Eds.; Wiley-VCH Verlag GmbH & Co. KGaA: Weinheim, 2004; p XIII.

$\boldsymbol{\sigma}$, were calculated using the EPR[80] and NMR[81–83] modules of the Amsterdam Density Functional (ADF) program package[84–88] and are tabulated in the Supporting Information. The Vosko–Wilk–Nusair[89] local density approximation with the Becke88-Perdew86[90–92] generalized gradient approximation were used for the exchange-correlation functional. ADF numerical integration parameters were increased from the default, 4.0, setting *accint* = 5.0 and *accsph* = 6.0 to better describe the core regions of the molecular orbitals. Scalar as well as scalar with spin–orbit relativistic corrections were carried out on the basis of the implementation of the zeroth order regular approximation, ZORA, formalism.[93–96] Triple-ζ doubly polarized, TZ2P, Slater-type ZORA basis sets were used for all atoms except for hydrogen, where double-ζ quality, DZ, basis functions were utilized. While the X-ray structures of the M[N(ⁱPr₂PSe)₂]₂ (M = Se, Te, Pt) complexes were used directly, optimized structures of Pd[N(ⁱPr₂PSe)₂]₂ as well as the chemical shift reference compounds were obtained using nonrelativistic ADF basis sets of comparable quality to those used in the magnetic shielding tensor calculations. Relativistic geometry optimizations were not performed due to a noted energy-potential mismatch in the ZORA approach.[88] The optimized structure of Pd[N(ⁱPr₂PSe)₂]₂ converged at a complex very similar to the platinum analogue (Figure 1b), an expected result given that the palladium and platinum complexes of the phenyl-derivatized ligand, M[N(Ph₂PSe)₂]₂ (M = Pd, Pt), are known to be isostructural.[6,7] The corresponding calculated chemical shift tensors were obtained from the magnetic shielding tensors using the relationship

$$\delta_{ii}(\text{sample}) = \frac{\sigma_{iso}(\text{ref}) - \sigma_{ii}(\text{sample})}{1 - \sigma_{iso}(\text{ref})} \quad (1)$$

where σ_{iso}(ref) is the isotropic shielding of a standard reference. The absolute shielding scale for ^{31}P has been determined, and the value of σ_{iso}(85% $H_3PO_{4(aq)}$) is 328.35 ppm.[97] Magnetic shielding calculations on optimized structures of the selenium, tellurium, and platinum reference compounds, dimethyl selenide, dimethyl telluride, and the hexachloroplatinate anion, respectively, have been performed; however, as solvent and vibrational effects have been omitted, the calculations serve only as a qualitative understanding of the chemical shift tensors obtained. We have previously investigated the selenium chemical shift tensors in a wide range of compounds and found the absolute isotropic magnetic shielding constant for a neat liquid of dimethyl selenide at 23 °C to be 1580 ppm for calculations with scalar relativistic corrections (hereafter denoted SC) included and 1745 ppm for calculations including scalar with spin–orbit relativistic corrections (hereafter SO).[98] Using a similar method, σ_{iso}(ref) = 2352 ppm (SC) and 3060 ppm (SO) were calculated for the absolute Te shielding from a nonrelativistically optimized structure of Me_2Te, in good agreement with an earlier study of calculated ^{125}Te chemical shifts.[99] The absolute Pt shieldings, σ_{iso}(ref), were calculated on an optimized structure of $[PtCl_6]^{2-}$, yielding values of −3471 ppm (SC) and −338 ppm (SO).

Results and Discussion

The square-planar complexes investigated, M[N(ⁱPr₂PSe)₂]₂ (M = Pd, Pt; Se, Te) as determined by computational chemistry or X-ray crystallography, display distinct structures depending on the central atom. The selenium and tellurium square-planar complexes are isostructural possessing a step-like structure with approximate 90° angles between the SePNPSe planes and the MSe_4 plane, whereas in the palladium and platinum complexes, the SePNPSe planes are considerably closer to coplanar with the MSe_4 plane (Figure 1). The MSe_2P_2N heterocycles for the Pd(II) and Pt(II) complexes possess a pseudoboat conformation; however, the six-membered rings of the Se(II) and Te(II) complexes have a distorted-chair conformation. Symmetry elements within each presented square-planar complex impose magnetic equivalence on two pairs of phosphorus and selenium environments, and as a result, only two unique phosphorus and selenium sites are expected in the corresponding solid-state NMR spectra. The results of the solid-state ^{31}P NMR investigation of the M[N(ⁱPr₂PSe)₂]₂ (M = Pd, Pt; Se, Te) complexes will be presented first, followed by the results of the solid-state ^{77}Se NMR spectra from the diselenoimidodiphosphinato selenium environments of the square-planar complexes. Finally the parameters from the solid-state ^{77}Se, ^{125}Te, and ^{195}Pt NMR investigation for the central atom will be discussed. In each case, the results for the traditional transition metal square-planar complexes will be presented first, followed by those for the main-group square-planar complexes highlighting any observed differences.

Solid-State ^{31}P NMR. The solid-state ^{31}P NMR spectra for M[N(ⁱPr₂PSe)₂]₂ (M = Pd, Pt) are given in Figure 2 along with their simulations. In each of these samples there exists a small impurity evident in the solid-state ^{31}P NMR spectra. The presence of these impurities did not hamper the spectral analysis, and no impurities were detected in the subsequent ^{77}Se and ^{195}Pt NMR investigations (vide infra), and thus, no effort was made to remove the impurity within the sample. The phosphorus chemical shift tensor parameters obtained are summarized in Table 1, along with estimations for the one-bond indirect selenium–phosphorus coupling constant, $^1J(^{77}Se,^{31}P)_{iso}$, from the observed satellite peaks in the ^{31}P NMR spectra. The isotropic chemical shifts and $^1J(^{77}Se,^{31}P)_{iso}$ values agree well with those measured for chloroform solutions: 55.9 ppm and 590 Hz for the palladium complex

(80) Schreckenbach, G.; Ziegler, T. *J. Phys. Chem. A* **1997**, *101*, 3388–3399.
(81) Schreckenbach, G.; Ziegler, T. *J. Phys. Chem.* **1995**, *99*, 606–616.
(82) Schreckenbach, G.; Ziegler, T. *Int. J. Quantum Chem.* **1997**, *61*, 899–918.
(83) Wolff, S. K.; Ziegler, T. *J. Chem. Phys.* **1998**, *109*, 895–905.
(84) Baerends, E. J.; Ellis, D. E.; Ros, P. *Chem. Phys.* **1973**, *2*, 41–51.
(85) Versluis, L.; Ziegler, T. *J. Chem. Phys.* **1988**, *88*, 322–328.
(86) te Velde, G.; Baerends, E. J. *J. Comput. Phys.* **1992**, *99*, 84–98.
(87) Fonseca Guerra, C.; Snijders, J. G.; te Velde, G.; Baerends, E. J. *Theor. Chem. Acc.* **1998**, *99*, 391–403.
(88) Theoretical Chemistry, Vrije Universiteit, Amsterdam, http://www.scm.com.
(89) Vosko, S. H.; Wilk, L.; Nusair, M. *Can. J. Phys.* **1980**, *58*, 1200–1211.
(90) Becke, A. D. *Phys. Rev. A* **1988**, *38*, 3098–3100.
(91) Perdew, J. P. *Phys. Rev. B* **1986**, *33*, 8822–8824.
(92) Perdew, J. P. *Phys. Rev. B* **1986**, *34*, 7406.
(93) Chang, C.; Pelissier, M.; Durand, P. *Phys. Scr.* **1986**, *34*, 394–404.
(94) van Lenthe, E.; Baerends, E. J.; Snijders, J. G. *J. Chem. Phys.* **1993**, *99*, 4597–4610.
(95) van Lenthe, E.; Baerends, E. J.; Snijders, J. G. *J. Chem. Phys.* **1994**, *101*, 9783–9792.
(96) van Lenthe, E.; van Leeuwen, R.; Baerends, E. J.; Snijders, J. G. *Int. J. Quantum Chem.* **1996**, *57*, 281–293.
(97) Jameson, C. J.; de Dios, A.; Jameson, A. K. *Chem. Phys. Lett.* **1990**, *167*, 575–582.
(98) Demko, B. A.; Eichele, K.; Wasylishen, R. E. *J. Phys. Chem. A* **2006**, *110*, 13537–13550.
(99) Ruiz-Morales, Y.; Schreckenbach, G.; Ziegler, T. *J. Phys. Chem. A* **1997**, *101*, 4121–4127.

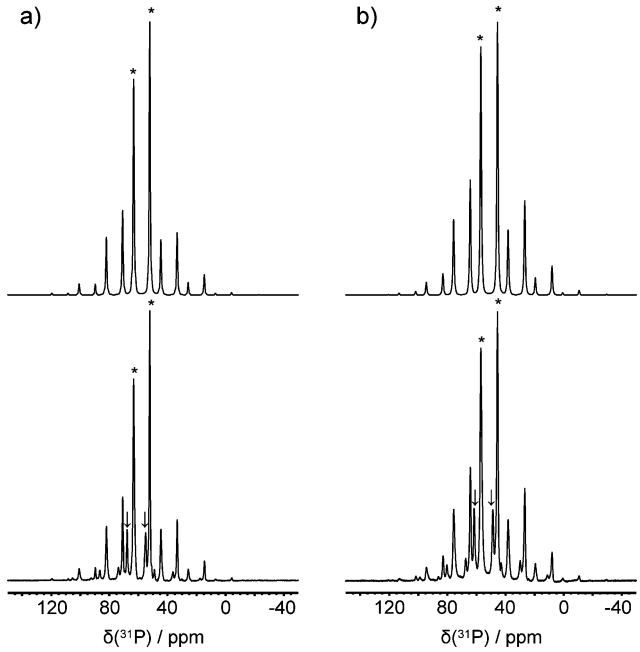

Figure 2. (a) VACP MAS ^{31}P NMR spectrum (lower trace) for Pd[N(^{i}Pr$_2$PSe)$_2$]$_2$ and its simulation (upper trace). (b) VACP MAS ^{31}P NMR spectrum (lower trace) for Pt[N(^{i}Pr$_2$PSe)$_2$]$_2$ and its simulation (upper trace). Experimental conditions: 11.7 T, 128 scans, MAS at 3.8 kHz, 5 Hz of line broadening, a 3.0 ms contact time, and a 9 s recycle delay. The isotropic peaks are marked with an asterisk (*), while those of impurities are marked with arrows (↓).

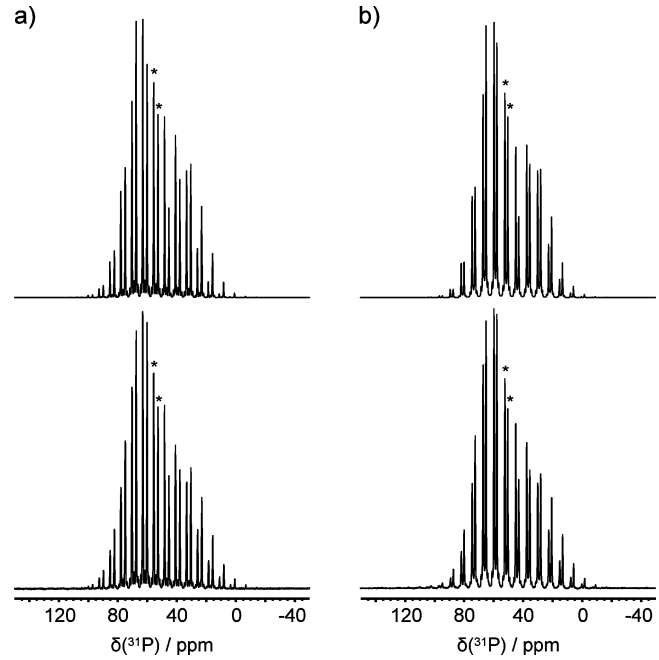

Figure 3. (a) VACP MAS ^{31}P NMR spectrum (lower trace) for Se[N(^{i}Pr$_2$PSe)$_2$]$_2$ and its simulation (upper trace). (b) VACP MAS ^{31}P NMR spectrum (lower trace) for Te[N(^{i}Pr$_2$PSe)$_2$]$_2$ and its simulation (upper trace). Experimental conditions: 11.7 T, 128 scans, MAS at 1.5 kHz, 5 Hz of line broadening, a 3.0 ms contact time, and a 9 s recycle delay. The isotropic peaks are marked with an asterisk (*).

Table 1. Experimental and Theoretical Solid-State ^{31}P NMR Parameters for M[N(^{i}Pr$_2$PSe)$_2$]$_2$ (M = Pd, Pt; Se, Te)

M^{II}	δ_{iso} (ppm)	δ_{11} (ppm)	δ_{22} (ppm)	δ_{33} (ppm)	Ω (ppm)	$^1J(^{77}Se,^{31}P)_{iso}$[a] (Hz)
Pd						
expt[b]	52.1	78.4	58.8	19.3	59.1	−520
	63.3	92.5	64.3	33.0	59.5	−520
SC	107.2	150.6	111.2	59.7	90.9	
	119.2	185.7	101.2	70.8	114.9	
SO	67.4	90.0	82.5	29.8	60.2	
	84.3	125.9	76.8	50.1	75.8	
Pt						
expt[b]	45.6	78.4	49.5	8.9	69.5	−480
	57.0	86.0	60.2	24.6	61.4	−480
SC	95.3	140.1	94.8	51.0	89.1	
	112.1	178.1	82.0	76.1	102.0	
SO	51.1	80.6	59.4	13.2	67.4	
	73.4	109.0	73.9	37.3	71.7	
Se						
expt[c]	52.8	82.3	63.7	12.3	70.0	−520
	55.7	84.1	59.2	23.6	60.5	−540
SC	115.0	162.1	111.7	71.2	90.8	
	118.6	159.1	120.1	76.6	82.4	
SO	56.0	89.2	63.3	15.6	73.6	
	58.4	88.3	62.9	23.8	64.4	
Te						
expt[c]	50.1	77.7	61.0	11.5	66.2	−500
	52.0	80.2	57.0	18.9	61.3	−530
SC	89.8	127.0	89.1	56.4	70.6	
	91.3	134.4	89.4	50.2	84.2	
SO	53.8	79.4	60.5	21.4	58.0	
	55.2	85.9	64.5	15.0	70.9	

[a] For directly bonded selenium-77 and phosphorus-31 spin pairs, signs of $^1J(^{77}Se,^{31}P)_{iso}$ are known to be negative for numerous analogous systems.[133,134] Estimated errors of $^1J(^{77}Se,^{31}P)_{iso}$ are ±10–20 Hz. [b] Estimated errors in δ_{ii} are ±1.2 ppm. [c] Estimated errors in δ_{ii} are ±0.8 ppm.

and 50.1 ppm and 536 Hz for the platinum complex.[8] Increasingly shielded phosphorus environments as the complexing metal becomes heavier have previously been reported for the tetraisopropyldiselenoimidodiphosphinato group 12 complexes, M[N(^{i}Pr$_2$PSe)$_2$]$_2$ (M = Zn, Cd, Hg).[67] The spans of the phosphorus chemical shift tensors (≤70 ppm) are small, indicating a more symmetric electronic environment than those found in trisorganophosphine selenides, whose average Ω is 124 ppm.[100] The DFT calculations are insufficiently accurate for definitive assignments of ^{31}P resonances to specific phosphorus sites within the respective crystal structures. The SC DFT calculations overestimate the isotropic ^{31}P chemical shifts as well as the principal components, δ_{ii}; however, calculated phosphorus chemical shift tensors that include the SO term achieve much better agreement with the experimental values, Table 1. Given the similarity of the principal components of the ^{31}P chemical shift tensors observed experimentally for the palladium and platinum complexes, it is not surprising that the tensors have similar calculated orientations for all of the phosphorus environments. The direction of δ_{11} is oriented perpendicular to the local Se−P−N plane, while δ_{33} lies approximately parallel to the phosphorus−nitrogen bond axis. The intermediate principal component, δ_{22}, nearly bisects the Se−P−N angle. Similar orientations have been calculated for the phosphorus chemical shift tensors in M[N(^{i}Pr$_2$PSe)$_2$]$_2$ (M = Zn, Cd, Hg) complexes.[67]

The corresponding ^{31}P VACP MAS spectra for the M[N(^{i}Pr$_2$PSe)$_2$]$_2$ (M = Se, Te) complexes are given in Figure 3. The isotropic chemical shifts and $^1J(^{77}Se,^{31}P)_{iso}$ values obtained are in agreement with the chloroform solution ^{31}P NMR values of 69.9 ppm and 526 Hz[3] and 58.7 ppm and 528 Hz[4] for the selenium and tellurium complexes, respec-

(100) Robert, J. B.; Wiesenfeld, L. *Mol. Phys.* **1981**, *44*, 319–327.

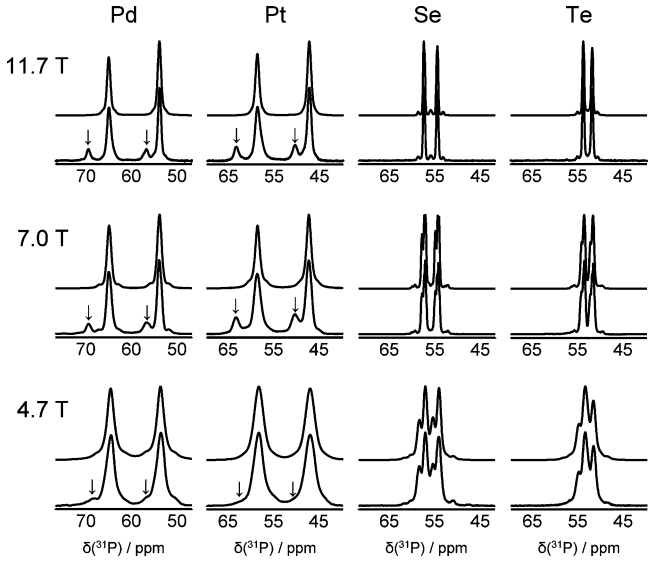

Figure 4. Experimental (lower trace) isotropic ^{31}P NMR regions, with spinning sidebands added to the isotropic region, and simulated (upper trace) for M[N(ⁱPr₂PSe)₂]₂ (M = Pd, Pt; Se, Te) at 4.7 T, 7.0 T, and 11.7 T. The isotropic peaks of the impurities are marked with arrows (↓).

tively. Similar values of $\delta_{iso}(^{31}P)$ and $\Omega(^{31}P)$ to those found in the Pd(II) and Pt(II) complexes are obtained, as well as a slight increase in phosphorus shieldings in the tellurium relative to the selenium complex. The SC calculated phosphorus chemical shift tensors are also overestimated for the Se(II) and Te(II) complexes, whereas the SO calculations again achieve improved agreement with experimental values. The orientations found at both the SC and SO levels are nearly identical to those described for the Pd(II) and Pt(II) complexes.

The principal difference observed between the transition-metal and main-group square-planar complexes is apparent in the ^{31}P NMR spectra at lower applied magnetic fields. Figure 4 displays the isotropic ^{31}P regions for the four complexes at 4.7, 7.0, and 11.7 T. While the two unique phosphorus environments are readily discernible for all four complexes in the isotropic region of the spectra obtained at 11.7 T, the spectra for the selenium and tellurium complexes obtained at the lower magnetic fields show significant fine structure as well as line broadening. The line shapes observed at 4.7 and 7.0 T result from the adjacent ^{14}N ($I = 1$, N.A. = 99.6%), which has previously been shown to influence solid-state ^{31}P NMR spectra of M[N(ⁱPr₂PSe)₂]₂ (M = Zn, Cd, Hg) complexes.[67] The energy levels of nitrogen-14 are quantized by both the applied magnetic field as well as the electric field gradient, EFG, at the ^{14}N nucleus.[101–103] As a result, MAS cannot completely average the dipolar interaction between ^{14}N and ^{31}P and "residual dipolar coupling" effects between the two nuclei are manifested in solid-state ^{31}P NMR spectra. This broadening effect is inversely proportional to the Larmor frequency of the quadrupolar nucleus, $\upsilon_N = \gamma_N B_0/2\pi$,[101–103] and thus produces a smaller effect at higher applied magnetic fields.

Analyses of these ^{31}P NMR spectra can yield values of the effective dipolar coupling constant, R_{eff}, and the isotropic indirect spin–spin coupling constant, $^1J(^{31}P,^{14}N)_{iso}$, as well as parameters describing the EFG at the nitrogen nucleus. The direct dipolar coupling constant, R_{DD}, is related to R_{eff} by

$$R_{eff} = R_{DD} - \Delta J/3 \qquad (2)$$

where $\Delta J = J_{33} - (J_{11} + J_{22})/2$ is the anisotropy of the phosphorus−nitrogen J-tensor, and

$$R_{DD} = \left(\frac{\mu_0}{4\pi}\right)\left(\frac{\hbar}{2\pi}\right)\left(\frac{\gamma_P\gamma_N}{\langle r_{PN}^3\rangle}\right) \qquad (3)$$

where μ_0 is the permeability of a vacuum, γ_P and γ_N are the magnetogyric ratios of ^{31}P and ^{14}N, and $<r_{PN}^3>$ is the motionally averaged cube of the distance between phosphorus and nitrogen.[104,105] The contributions from ΔJ are expected to be negligible given the small magnitude for $^1J(^{31}P,^{15}N)_{iso}$ determined for iminobis(diphenylphosphine selenide), HN(Ph₂PSe)₂,[106] and similarly small values of $^1J(^{31}P,^{14}N)_{iso}$ found previously for the group 12 complexes of $[N(^iPr_2PSe)_2]^-$.[67] As a result, R_{eff} can be estimated directly from the phosphorus−nitrogen nuclear separation determined by X-ray diffraction. It is not possible to assign a specific R_{DD}, i.e., a specific phosphorus−nitrogen distance, to a specific ^{31}P NMR resonance, so an average r_{PN} was calculated from the two P−N distances within each complex. The resulting average R_{DD} was used in the simulations for both sites in the ^{31}P NMR spectra. The quadrupolar parameters required to describe the solid-state NMR spectrum of a spin-½ nucleus spin–spin coupled to a quadrupolar nucleus is the quadrupolar coupling constant, $C_Q = eQV_{ZZ}/h$, where e is the elementary charge, Q is the nuclear quadrupole moment, and V_{ZZ} is the largest component of the EFG tensor at the nucleus. Also required are the Euler angles, α and β, which describe the orientation of the dipolar vector, r_{PN}, within the principal axis system of the EFG tensor at the quadrupolar nucleus. Preliminary values of C_Q, as well as the angles α and β used herein were obtained from DFT calculations of the nitrogen EFG tensors. For reasons analogous to those given above for R_{DD}, the simulations of both phosphorus lineshapes in each spectrum were obtained using a single value of $^1J(^{31}P,^{14}N)_{iso}$, C_Q, α, and β. The effect of using single average values of the residual dipolar coupling parameters does not appear to significantly impair the quality of the simulations for the ^{31}P NMR spectra of the Se(II) and Te(II) complexes given in Figure 4, where accurate lineshapes are achieved at all three applied magnetic fields employed.

For Se[N(ⁱPr₂PSe)₂]₂, R_{DD} = 890(50) Hz was obtained from the average r_{PN} distance of 1.583(30) Å,[3] and the azimuthal and polar angles were 90(3)° and 18(5)°, respectively. The value of C_Q was 2.50(20) MHz, and the indirect spin–spin coupling constant, $^1J(^{31}P,^{14}N)_{iso}$, was 15(4) Hz. The parameters pertaining to residual dipolar coupling used in

(101) Olivieri, A. C. *J. Magn. Reson.* **1989**, *81*, 201–205.
(102) Zumbulyadis, N.; Henrichs, P. M.; Young, R. H. *J. Chem. Phys.* **1981**, *75*, 1603–1611.
(103) Hexem, J. G.; Frey, M. H.; Opella, S. J. *J. Chem. Phys.* **1982**, *77*, 3847–3856.

the simulations of the ^{31}P NMR spectra of Te[N(^{i}Pr$_2$PSe)$_2$]$_2$ were R_{DD} = 890(50) Hz, r_{PN} = 1.583(30) Å,[4] α = 90(3)°, β = 16(5)°, C_Q = 2.55(20) MHz, and $^1J(^{31}P,^{14}N)_{iso}$ = 16(5) Hz. These residual dipolar coupling parameters are consistent with those found in other diselenoimidodiphosphinate complexes,[67] and the magnitude of the quadrupolar coupling constants obtained are reasonable in comparison with other phosphorus−nitrogen systems where values of C_Q are not expected to exceed 4.0 MHz.[107] The EFG tensors at ^{14}N in the selenium and tellurium complexes are oriented similarly, such that the largest component, V_{ZZ}, lies within the P−N−P plane perpendicular to the P−N−P bisector, the intermediate component is parallel to the direction of the formal electron "lone pair" on the nitrogen, and the smallest EFG component is perpendicular to the P−N−P plane. In contrast, the calculated ^{14}N EFG tensors for the palladium and platinum complexes, despite possessing similar calculated quadrupolar coupling constants to those in the Se(II) and Te(II) complexes, are oriented such that it is the largest component that is perpendicular to the P−N−P plane, and the smallest EFG component within the P−N−P plane perpendicular to the P−N−P bisector. Such a tensor results in values of 25° for α, and 90° for β, which would not produce discernible fine structure in the ^{31}P MAS lineshapes due to residual dipolar coupling from nitrogen even at low magnetic field strengths.

Solid-State ^{77}Se NMR Results of the Diselenoimidodiphosphinato Selenium Environments. The entire spinning-side band manifolds for the solid-state ^{77}Se NMR spectra obtained for the transition-metal square-planar complexes investigated at 7.0 T are given in Figure 5. The solid-state NMR parameters obtained from simulations of the spectra for the diselenoimidodiphosphinato selenium environments are detailed in Table 2. Differences in the relative intensities of the respective *J*-coupled spectra were insufficient for the extraction of meaningful values of the selenium−phosphorus coupling parameters, R_{eff} and ΔJ. The ^{77}Se NMR parameters for the palladium and platinum complexes are very similar with isotropic chemical shifts that are all within 20 ppm, indicating very comparable selenium environments considering that the selenium chemical shift range exceeds 3000 ppm.[108,109] The solid-state ^{77}Se NMR spectra of the group 12 complexes, M[N(^{i}Pr$_2$PSe)$_2$] (M = Zn, Cd, Hg), also shows little variation in the selenium chemical shift parameters between the selenium sites present in those complexes.[67] Theoretical calculations of the selenium chemical shift tensors reproduce the experimental values well (Table 2). The obtained indirect selenium−phosphorus coupling, $^1J(^{77}Se,^{31}P)_{iso}$, values of −485 and −560 Hz for Pd[N(^{i}Pr$_2$PSe)$_2$]$_2$ agree well with the single value obtained from solution ^{31}P NMR, 590 Hz,[8] and the values determined from the ^{31}P solid-state NMR spectra (Table 1). Similarly for the Pt(II) complex, the $^1J(^{77}Se,^{31}P)_{iso}$ values of −450 and −510

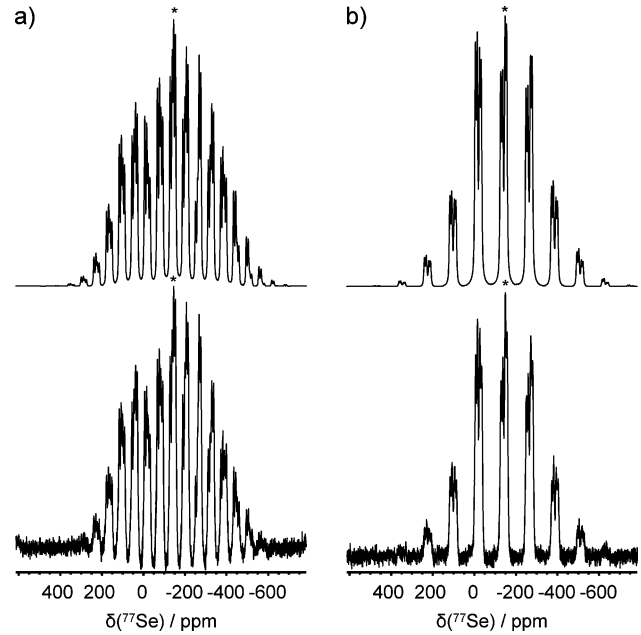

Figure 5. (a) VACP MAS ^{77}Se NMR spectra for Pd[N(^{i}Pr$_2$PSe)$_2$]$_2$. Experimental conditions: 7.0 T, 30128 scans, spinning at 3.5 kHz, 20 Hz of line broadening, a 9.0 ms contact time, and an 8 s recycle delay. (b) VACP MAS ^{77}Se NMR spectra for Pt[N(^{i}Pr$_2$PSe)$_2$]$_2$. Experimental conditions: 7.0 T, 15560 scans, spinning at 7.0 kHz, 20 Hz of line broadening, a 10.0 ms contact time, and a 5 s recycle delay. Simulated spectra are shown in the upper traces. The isotropic peaks are marked with an asterisk (*).

Table 2. Experimental and Theoretical Solid-State ^{77}Se NMR Parameters for the Anion of M[N(^{i}Pr$_2$PSe)$_2$]$_2$ (M = Pd, Pt; Se, Te)

M^{II}	δ_{iso} (ppm)	δ_{11} (ppm)	δ_{22} (ppm)	δ_{33} (ppm)	Ω (ppm)	$^1J(^{77}Se,^{31}P)_{iso}$[a] (Hz)	$^1J(M,^{77}Se)_{iso}$ (Hz)
Pd							
expt[b]	−133	228	−92	−536	764	−560	
	−150	195	−194	−450	645	−485	
SC	55	447	113	−395	842		
	47	399	−22	−236	635		
SO	48	422	142	−421	843		
	30	356	−23	−244	600		
Pt							
expt[b]	−132	209	−102	−502	711	−510	
	−152	170	−152	−475	645	−450	
SC	−28	335	41	−459	794		
	−24	320	−52	−342	662		
SO	−42	283	28	−436	719		
	−49	263	−72	−337	600		
Se							
expt[c]	120	383	108	−131	514	−520	±405
	32	333	14	−250	583	−535	±435
SC	178	558	188	−211	769		
	111	563	132	−363	926		
SO	120	500	82	−223	723		
	58	488	34	−347	835		
Te							
expt[c]	−11	162	24	−219	381	−520	±1120
	−105	163	−152	−327	490	−540	±1270
SC	−17	174	23	−248	422		
	−78	232	−97	−368	600		
SO	−18	207	−5	−255	461		
	−81	232	−123	−353	586		

[a] For directly bonded selenium-77 and phosphorus-31 spin pairs, signs of $^1J(^{77}Se,^{31}P)_{iso}$ are known to be negative for numerous analogous systems.[133,134] Estimated errors of $^1J(^{77}Se,^{31}P)_{iso}$ are ±5–10 Hz. [b] Estimated errors in δ_{ii} are ±14 ppm. [c] Estimated errors in δ_{ii} are ±8 ppm.

(104) Wasylishen, R. E. In *Encyclopedia of Nuclear Magnetic Resonance*; Grant, D. M., Harris, R. K., Eds.; John Wiley and Sons, Ltd.: Chichester, 1996; pp 1685–1695..
(105) Wasylishen, R. E. In *Encyclopedia of Nuclear Magnetic Resonance*; Grant, D. M., Harris, R. K., Eds.; John Wiley and Sons, Ltd.: Chichester, 2002; Vol. *9*, pp 274–282..
(106) Wrackmeyer, B.; Garcia-Baez, E.; Zuno-Cruz, F. J.; Sanchez-Cabrera, G.; Rosales, M. J. *Z. Naturforsch., B* **2000**, *55*, 185–188.
(107) Power, W. P.; Wasylishen, R. E.; Curtis, R. D. *Can. J. Chem.* **1989**, *67*, 454–459.
(108) Duddeck, H. *Prog. Nucl. Magn. Reson. Spectrosc.* **1995**, *27*, 1–323.
(109) Duddeck, H. *Annu. Rep. NMR Spectrosc.* **2004**, *52*, 105–166.

Hz are in agreement with the solid-state ^{31}P NMR value above, and the magnitude from a chloroform solution ^{31}P NMR spectrum of Pt[N(^{i}Pr$_2$PSe)$_2$]$_2$, 536 Hz.[8] There was no evidence of $^1J(^{195}\text{Pt},^{77}\text{Se})_{iso}$ in the solid-state ^{77}Se NMR spectrum of Pt[N(^{i}Pr$_2$PSe)$_2$]$_2$. This prompted us to investigate the complex via solution ^{77}Se NMR yielding an isotropic chemical shift of −137 ppm consistent with the solid-state values in Table 2, and a $^1J(^{195}\text{Pt},^{77}\text{Se})_{iso}$ value of 90 Hz, which is well within the obtained linewidths in the corresponding solid-state ^{77}Se NMR spectrum. Calculated orientations of selenium magnetic shielding tensors for trisorganophosphine selenide compounds, R_3PSe, were found to be sensitive to the nature of the R group.[98] However, the selenium magnetic shielding tensors for the transition metal complexes, as determined by the DFT calculations, possess similar orientations with the directions of δ_{11} and δ_{33}, oriented nearly parallel with the metal−selenium and selenium−phosphorus bond axes, respectively. The intermediate component, δ_{22}, is oriented perpendicular to the local M−Se−P plane.

The solid-state ^{77}Se NMR spectrum for the ligands of the Se[N(^{i}Pr$_2$PSe)$_2$]$_2$ complex overlaps with the spectrum for the central selenium atom; see Figure 6. The experimentally observed solid-state ^{77}Se NMR spectrum (Figure 6a) agrees well with the simulation of all selenium environments (Figure 6b), which comprises the simulations for the ligand (Figure 6c) and that of the central selenium atom (Figure 6d). The solid-state ^{77}Se NMR spectrum for Te[N(^{i}Pr$_2$PSe)$_2$]$_2$ at 7.0 T along with its simulation is given in parts e and f of Figure 6, respectively. The experimental solid-state ^{77}Se NMR parameters for the ligand for both of the main-group square-planar complexes are well reproduced by the DFT calculations, Table 2. The significant difference between the values of δ_{iso}(Se) for the two selenium sites within the Se(II) and Te(II) complexes, along with the consistent reproduction of this difference by the DFT computations, permits the assignment of these resonances to specific selenium environments within the M[N(^{i}Pr$_2$PSe)$_2$]$_2$ structures. For both main-group complexes, the site with the larger isotropic chemical shift corresponds to the selenium site within the crystal structure with smaller M−Se and Se−P distances, as well as smaller M−Se-P angle; whereas, the site with the smaller value of δ_{iso}(Se) corresponded to the selenium site with larger M−Se and Se−P distances and larger M−Se−P angle. The obtained $^1J(^{77}\text{Se},^{31}\text{P})_{iso}$ of −520 and −535 Hz for Se[N-(^{i}Pr$_2$PSe)$_2$]$_2$ agree well with the solution ^{31}P NMR magnitude of 526 Hz[3] and the solid-state ^{31}P NMR value given in Table 1. Additionally, the indirect spin–spin couplings obtained between the central selenium and the selenium nuclei from the ligands, $^1J(^{77}\text{Se},^{77}\text{Se})_{iso} = \pm 405$ and ± 435 Hz, obtained from the ∼7.63% relative intensity satellite peaks, are in good agreement with the magnitude of 391 Hz for selenium−selenium one-bond coupling in Se[Se$_2$CN(^{i}Bu)$_2$]$_2$,[110] which was previously recognized as the largest known value of $^1J(^{77}\text{Se},^{77}\text{Se})_{iso}$.[108] The $^1J(^{77}\text{Se},^{31}\text{P})_{iso}$ values for the tellurium complex, −520 and −540 Hz, are in agreement with our solid-state ^{31}P NMR value above, and the coupling observed from a chloroform solution, 528 Hz.[4] The magnitudes of $^1J(^{125}\text{Te},^{77}\text{Se})_{iso}$, 1120 and 1270 Hz, appear to be the largest tellurium−selenium couplings reported, over 500 Hz larger than those found in polychalcogenides.[111–113] Scaling of these $^1J(^{125}\text{Te},^{77}\text{Se})_{iso}$ and the values of $^1J(^{77}\text{Se},^{77}\text{Se})_{iso}$ for the Se(II) complex by $4\pi^2/h\gamma_M\gamma_{Se}$ yields the reduced coupling constants $^1K(\text{M,Se})_{iso}$, which allows for direct comparison. The values of $^1K(\text{Se,Se})_{iso}$, 918 × 10^{19} T^2 J^{-1} and 986 × 10^{19} T^2 J^{-1}, are of a similar order of magnitude yet smaller than the corresponding $^1K(\text{Te,Se})_{iso}$, 1529 × 10^{19} T^2 J^{-1} and 1734 × 10^{19} T^2 J^{-1}, found for Te[N(^{i}Pr$_2$PSe)$_2$]$_2$. Increasing magnitudes of $^1K(\text{M,Se})_{iso}$ as one moves down a group in the periodic table is a well-known trend for various group 14 couplings[114–120] and has also been observed in the coupling of the group 12 metal centers, cadmium and mercury, with selenium in diselenoimidodiphosphinato complexes.[67]

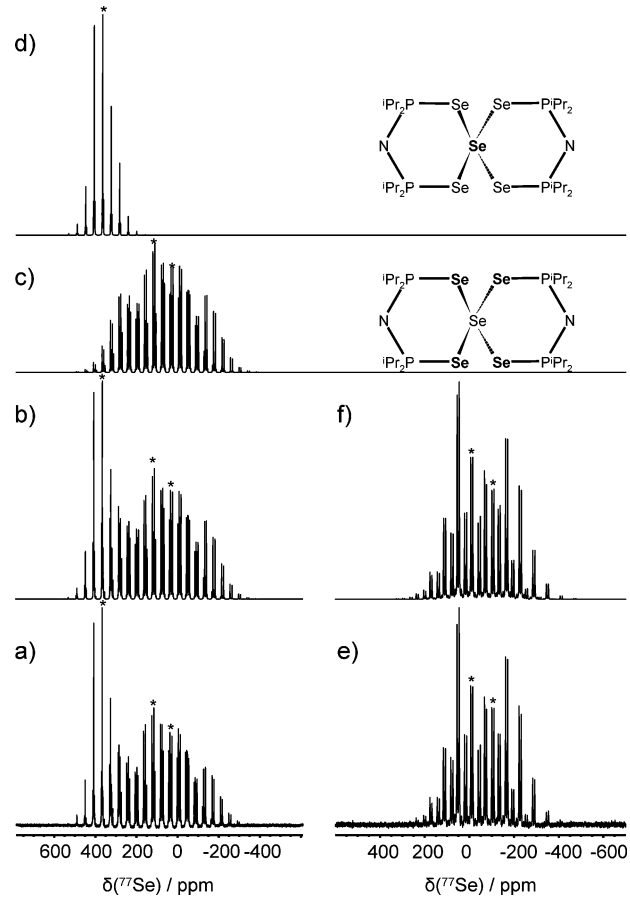

Figure 6. (a) Experimental VACP MAS ^{77}Se NMR spectrum for Se[N(^{i}Pr$_2$PSe)$_2$]$_2$. Experimental conditions: 7.0 T, 31808 scans, 5 Hz of line broadening, a 9.0 ms contact time, and a 5 s recycle delay. (b) Total simulation of all selenium environments for Se[N(^{i}Pr$_2$PSe)$_2$]$_2$. (c) Simulation of the ^{77}Se MAS spectrum for the anion of Se[N(^{i}Pr$_2$PSe)$_2$]$_2$. (d) Simulation of the ^{77}Se MAS spectrum for the central selenium in Se[N(^{i}Pr$_2$PSe)$_2$]$_2$. (e) VACP MAS ^{77}Se NMR spectrum for Te[N(^{i}Pr$_2$PSe)$_2$]$_2$. Experimental conditions: 7.0 T, 10896 scans, 10 Hz of line broadening, an 11.0 ms contact time, and an 8 s recycle delay. (f) Simulation of the ^{77}Se MAS spectrum for Te[N(^{i}Pr$_2$PSe)$_2$]$_2$. The isotropic peaks are marked with an asterisk (*).

(110) Mazaki, Y.; Kobayashi, K. *Tetrahedron Lett.* **1989**, *30*, 2813–2816.

(111) Schrobilgen, G. J.; Burns, R. C.; Granger, P. *J. Chem. Soc., Chem. Commun.* **1978**, 957–960.

(112) Björgvinsson, M.; Schrobilgen, G. J. *Inorg. Chem.* **1991**, *30*, 2540–2547.

(113) Björgvinsson, M.; Sawyer, J. F.; Schrobilgen, G. J. *Inorg. Chem.* **1991**, *30*, 4238–4245.

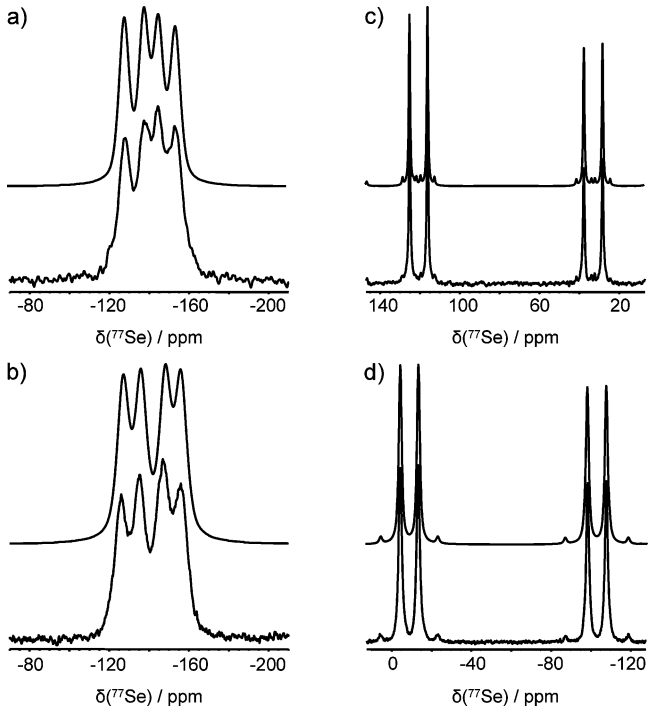

Figure 7. Expansion of the isotropic regions of the ^{77}Se NMR spectra at 7.0 T (lower trace) and the corresponding simulations (upper traces) for the diselenoimidodiphosphinate anion of the square-planar complexes $M[N(^iPr_2PSe)_2]_2$, M = (a) Pd, (b) Pt, (c) Se, (d) Te.

There are a number of notable differences between the solid-state ^{77}Se NMR parameters for the diselenoimidodiphosphinato selenium environments in the transition-metal square-planar complexes and those for the main-group complexes. The first observed difference involves the isotropic region of the ^{77}Se NMR spectra. It is readily apparent from Figure 7 that the isotropic shifts within the ^{77}Se NMR spectra of the Pd(II) (Figure 7a) and Pt(II) (Figure 7b) complexes are considerably closer together than those for the Se(II) (Figure 7c) and Te(II) (Figure 7d) complexes. While the selenium isotropic shifts of the transition-metal complexes are approximately 20 ppm apart, the ^{77}Se resonances for the main group square-planar complexes are nearly 90 ppm separated from each other. Additionally, the selenium chemical shifts for the transition metal complexes do not vary much when the complexing metal is changed from palladium to platinum, $\Delta\delta_{iso} \leq 2$ ppm; however, the isotropic ^{77}Se NMR peaks for the $[N(^iPr_2PSe)_2]^-$ selenium environments are separated by more than 130 ppm, depending on whether the central atom is selenium or tellurium (Table 2). Second, the spans of the selenium chemical shift tensors of the diselenoimidodiphosphinato selenium environments in the selenium and tellurium complexes are on the order of 200 ppm smaller than those for the transition-metal complexes; however, all spans of the selenium chemical shift tensors investigated are still larger than those typically found in tris-organophosphine selenides.[98,121] Finally, the calculated orientation of the $[N(^iPr_2PSe)]^-$ selenium chemical shift tensors depend on whether the complexing center is palladium and platinum or selenium and tellurium. For the main-group square planar complexes, δ_{33} is oriented nearly parallel to the metal−selenium bond axis, δ_{11} is approximately aligned with the selenium−phosphorus bond axis, with δ_{22} perpendicular to the local M−Se−P plane. These are distinctly different from the orientation of the selenium chemical shift tensors in the palladium and platinum complexes where δ_{11} was calculated parallel to the metal−selenium axis and δ_{33} parallel to the selenium−phosphorus axis. The difference in the magnitude of the spans and orientations of the selenium chemical shift tensors may be a result of the difference between the selenium environment being within a MSe_2P_2N heterocyclic ring with a distorted-chair conformation, M = Se or Te, rather than a pseudoboat conformation as seen above with the palladium and platinum complexes as well as previously observed for the tetraisopropyldiselenoimidodiphosphinato group 12 complexes, $M[N(^iPr_2PSe)_2]_2$ (M = Zn, Cd, Hg), which also possess similarly oriented selenium chemical shift tensors and spans greater than 650 ppm within their pseudoboat heterocyclic ring structures.[67]

Table 3. Experimental and Theoretical Solid-State NMR Parameters for $M[N(^iPr_2PSe)_2]_2$ (M = ^{195}Pt; ^{77}Se, ^{125}Te)

M^{II}	δ_{iso} (ppm)	δ_{11} (ppm)	δ_{22} (ppm)	δ_{33} (ppm)	Ω (ppm)	κ (ppm)	$^1J(M,^{77}Se)_{iso}$ (Hz)
Pd[a]							
SC	0	1801	−796	−1005	2806	−0.87	
SO	0	1866	−818	−1049	2915	−0.86	
Pt							
expt[b]	−4580	−2412	−5623	−5706	3294	−0.95	
SC	−6017	−4651	−6611	−6790	2146	−0.83	
SO	−6347	−4648	−7076	−7319	2671	−0.82	
Se							
expt[c]	367	457	389	255	202	0.32	±424
SC	296	523	245	119	404	−0.37	
SO	373	446	399	275	171	0.45	
Te							
expt[d]	645	1330	1073	−468	1798	0.71	±1200
SC	295	817	99	−30	848	−0.68	
SO	508	963	741	−179	1142	0.59	

[a] Pd-105 chemical shift tensors are given as a traceless representation. [b] Estimated errors in δ_{ii} are ±80 ppm. [c] Estimated errors in δ_{ii} are ±5 ppm. [d] Estimated errors in δ_{ii} are ±40 ppm.

Solid-State NMR of the Central Atom of $M[N(^iPr_2PSe)_2]_2$ (M = ^{195}Pt, ^{77}Se, ^{125}Te). The results of the solid-state ^{77}Se, ^{125}Te, and ^{195}Pt NMR investigation on the spin-½ nuclei of the central atoms in the $M[N(^iPr_2PSe)_2]_2$ (M = Pt; Se, Te) complexes are given in Table 3. Palladium-105 is a low-γ quadrupolar nucleus, $S = 5/2$, with a large quadrupolar moment, $Q = 66.0$ fm^2,[122] making it impractical to study at

(114) Dreeskamp, H.; Stegmeier, G. *Z. Naturforsch., A* **1967**, *22*, 1458–1464.
(115) Kennedy, J. D.; McFarlane, W.; Pyne, G. S.; Wrackmeyer, B. *Dalton Trans.* **1975**, 386–390.
(116) Kennedy, J. D.; McFarlane, W.; Wrackmeyer, B. *Inorg. Chem.* **1976**, *16*, 1299–1302.
(117) Wrackmeyer, B.; Horchler, K. *Magn. Reson. Chem.* **1990**, *28*, 56–61.
(118) Wrackmeyer, B.; Zhou, H. *Magn. Reson. Chem.* **1990**, *28*, 1066–1069.
(119) Christendat, D.; Butler, I. S.; Gilson, D. F. R.; Morin, F. G. *Can. J. Chem.* **1999**, *77*, 1892–1898.
(120) Willans, M. J.; Demko, B. A.; Wasylishen, R. E. *Phys. Chem. Chem. Phys.* **2006**, *8*, 2733–2743.
(121) Grossmann, G.; Potrzebowski, M. J.; Fleischer, U.; Krüger, K.; Malkina, O. L.; Ciesielski, W. *Solid State Nucl. Magn. Reson.* **1998**, *13*, 71–85.
(122) Harris, R. K.; Becker, E. D.; Crabral de Menezes, S. M.; Goodfellow, R.; Granger, P. *Pure Appl. Chem.* **2001**, *73*, 1795–1818.

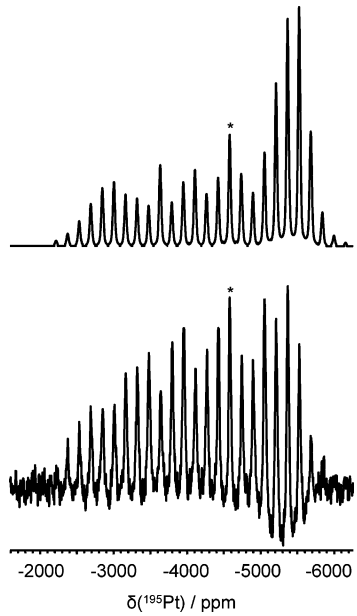

Figure 8. VACP MAS ^{195}Pt NMR spectrum of Pt[N(^{i}Pr$_2$PSe)$_2$]$_s$ (lower trace) and its simulation (upper trace). Experimental conditions: 4.7 T, 84656 scans, spinning at 6.75 kHz, 200 Hz of line broadening, a 10.0 ms contact time, and a 9 s recycle delay. The isotropic peak is marked with an asterisk (*).

the moderate magnetic fields employed; however, DFT computations of the ^{105}Pd chemical shift tensor were performed and are included in Table 3. The solid-state ^{195}Pt NMR spectrum of Pt[N(^{i}Pr$_2$PSe)$_2$]$_2$ at 4.7 T is given in Figure 8 along with its simulation. The isotropic ^{195}Pt chemical shift, −4580 ppm, agrees well with the solution ^{195}Pt NMR value, −4308 ppm, as well as that for the phenyl-derivated complex, Pt[N(Ph$_2$PSe)$_2$]$_2$, −4240 ppm.[6,7] The broad spectrum spanning over 3000 ppm affords rather low resolution, and provides no evidence for splittings due to platinum−selenium coupling; however, the solution-state ^{195}Pt NMR spectrum displays a $^{1}J(^{195}\text{Pt},^{77}\text{Se})_{iso}$ of 92 Hz consistent with the solution-state ^{77}Se NMR value, as well as a $^{2}J(^{195}\text{Pt},^{31}\text{P})_{iso}$ value of 94 Hz. Despite being of a similar order of magnitude with other platinum−selenium couplings,[108] the small value of $^{1}J(^{195}\text{Pt},^{77}\text{Se})_{iso}$ was unexpected given the large $^{1}J(^{125}\text{Te},^{77}\text{Se})_{iso}$ couplings observed herein for Te[N(^{i}Pr$_2$PSe)$_2$]$_2$, ± 1120 and ± 1270 Hz, as well as the $^{1}J(^{199}\text{Hg},^{77}\text{Se})_{iso}$ values found for Hg[N(^{i}Pr$_2$PSe)$_2$]$_2$ ranging from −850 to −900 Hz.[67]

The principal components of the palladium and platinum chemical shift tensors indicate nearly axially symmetric environments about the central transition-metal centers in M[N(^{i}Pr$_2$PSe)$_2$]$_2$, M = Pd, Pt, consistent with experimental ^{195}Pt chemical shift tensors observed in other square-planar platinum complexes.[123–126] Orbital interpretations of paramagnetic shielding contributions have been successful in

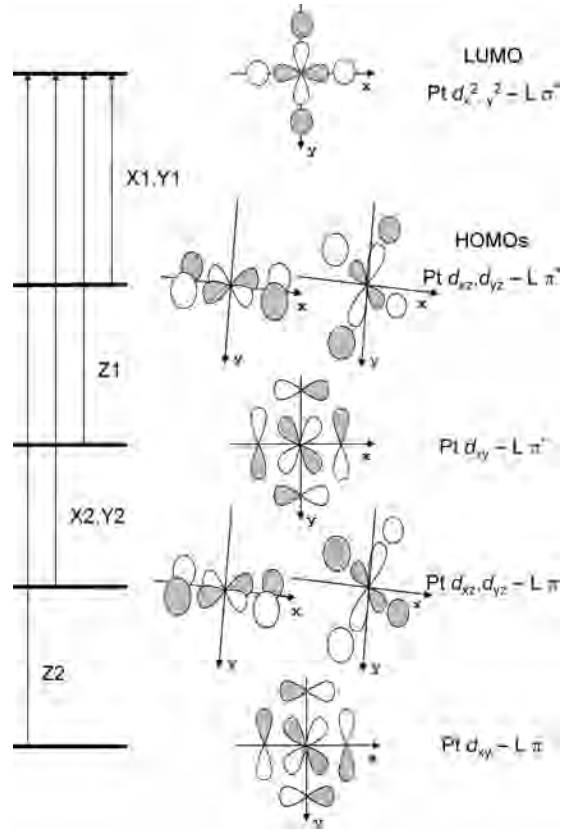

Figure 9. Molecular orbital diagram for an idealized Pt^{II}L$_4$ anion adapted from ref 129. X and Y magnetic-dipole allowed mixing lead to paramagnetic contributions within the square plane; whereas, Z mixing lead to deshielding contributions perpendicular to the molecular plane.

understanding the physical origin of the observed chemical shift tensors for numerous molecular systems.[127,128] Gilbert and Ziegler have utilized qualitative molecular orbital theory along with ZORA DFT calculations to describe the ^{195}Pt shielding environments for several square-planar platinum complexes.[129] Their results show that platinum chemical shift tensors with negative skews (i.e., $\delta_{22} \approx \delta_{33}$) arise from large deshielding paramagnetic contributions perpendicular to the square plane resulting from the magnetic-dipole allowed mixing of $d_{xy} \rightarrow d_{x^2-y^2}$; occupied → virtual orbital mixing, Z1 and Z2 in Figure 9.[129] The SC and SO calculated platinum chemical shift tensors for Pt[N(^{i}Pr$_2$PSe)$_2$]$_2$ are in fair agreement with experiment given that the ^{195}Pt chemical shift range covers 13000 ppm.[130] The discrepancy between the calculations suggests that scalar ZORA relativistic corrections are not completely able to detail the local platinum environment. The inclusion of spin–orbit relativistic corrections yield better agreement, indicating that these effects are important for describing the local environment of this heavy transition metal. The calculations do however perform well in describing the shape and size of the platinum chemical shift tensor,

(123) Harris, R. K.; McNaught, I. J.; Reams, P.; Packer, K. J. *Magn. Reson. Chem.* **1991**, *29*, S60–S72.
(124) Harris, R. K.; Reams, P.; Packer, K. J. *Dalton Trans.* **1986**, 1015–1020.
(125) Austin, E. J.; Barrie, P. J.; Clark, R. J. H. *Chem. Commun.* **1993**, 1404–1405.
(126) Duer, M. J.; Khan, M. S.; Kakkar, A. K. *Solid State Nucl. Magn. Reson.* **1992**, *1*, 13–16.
(127) Jameson, C. J.; Gutowsky, H. S. *J. Chem. Phys.* **1964**, *40*, 1714–1724.
(128) Grutzner, J. B. In *Recent Advances in Organic NMR Spectroscopy*; Lambert, J. B., Rittner, R., Eds.; Norell Press: Landsville, NJ, 1987; pp 17–42..
(129) Gilbert, T. M.; Ziegler, T. *J. Phys. Chem. A* **1999**, *103*, 7535–7543.
(130) Still, B. M.; Kumar, P. G. A.; Aldrich-Wright, J. R.; Prize, W. S. *Chem. Soc. Rev.* **2007**, *36*, 665–686.

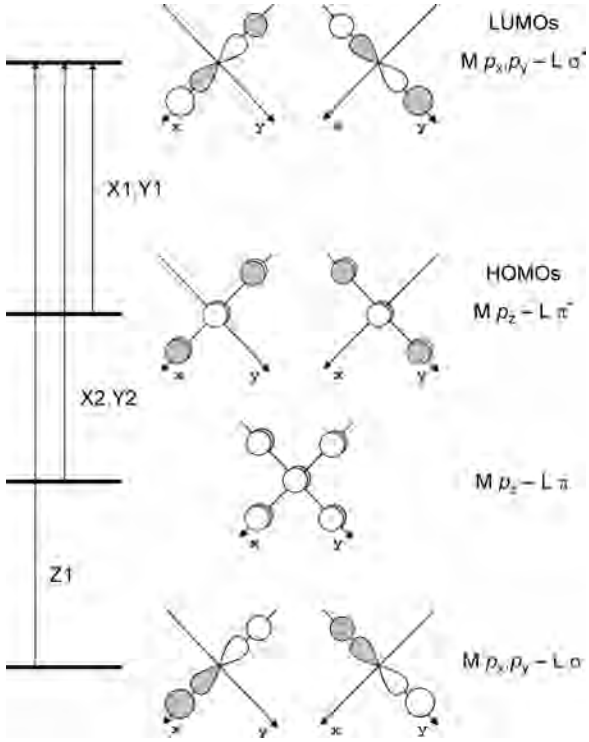

Figure 10. Molecular orbital diagram for an idealized $M^{II}L_4$ (M = Se, Te) anion. X and Y magnetic-dipole allowed mixing lead to paramagnetic contributions within the square plane, whereas Z mixing lead to deshielding contributions perpendicular to the molecular plane.

as shown in the comparable values of the skew and magnitudes of the span, see Table 3. The calculated orientation of the platinum chemical shift tensor also correctly predicts a nearly axially symmetric tensor, suggesting that directions of δ_{33} and δ_{22} are coincident within the $PtSe_4$ plane and that δ_{11} is oriented perpendicular to the square plane.

The solid-state ^{77}Se NMR spectrum for $Se[N(^iPr_2PSe)_2]_2$ at 7.0 T is shown in Figure 6. The simulation of the central selenium site (Figure 6d) shows a selenium chemical shift tensor that possesses a considerably smaller span than the ligand selenium environments, Figure 6c and Tables 2 and 3. The isotropic ^{77}Se chemical shift, 367 ppm, is consistent with those found in other selenium(II) centers,[110,131] and the observed $^1J(^{77}Se,^{77}Se)_{iso}$, ± 424 Hz, obtained from the 4 × 7.63% = 30.52% relative intensity satellite peaks, is in good agreement with the indirect one-bond selenium−selenium coupling constants found from the diselenoimidodiphosphinato selenium environments within the same spectrum given in Table 2. The small span, positive skew, and nonaxially symmetric ^{77}Se chemical shift tensor are in stark contrast to the corresponding platinum chemical shift tensor for $Pt[N(^iPr_2PSe)_2]_2$, with its large span, near-axial symmetry, and negative κ. The difference between the skews of the respective central selenium and platinum chemical shift tensors can also be understood via qualitative molecular orbital theory. Figure 10 displays the dominant magnetic-dipole allowed mixing of orbitals, obtained using the EPR module from the DFT computations, for describing the

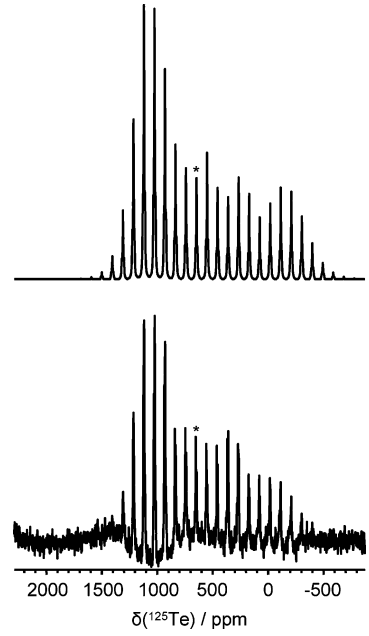

Figure 11. VACP MAS ^{125}Te NMR spectrum of $Te[N(^iPr_2PSe)_2]_x$ (lower trace) and its simulation (upper trace). Experimental conditions: 4.7 T, 25616 scans, spinning at 6.0 kHz, 100 Hz of line broadening, a 8.0 ms contact time, and a 20 s recycle delay. The isotropic peak is marked with an asterisk (*).

shielding for the central atom within the main-group square-planar complexes investigated. Deshielding paramagnetic contributions arise within the molecular square plane due to $p_z \rightarrow p_{x,y}$ mixing (X1,Y1 and X2,Y2 in Figure 10), whereas the majority of the deshielding perpendicular to the plane results from the $p_{x,y}$(occupied) $\rightarrow p_{y,x}$(virtual) mixing (Z1 in Figure 10). Since the paramagnetic contributions from the X1,Y1 and X2,Y2 mixing are larger than those from Z1, the principal components approximately within the $SeSe_4$ plane are more deshielded than the component perpendicular to the plane and a chemical shift tensor with a positive skew is found. The scalar relativistic calculated selenium chemical shift tensor has difficulty reproducing all of the experimental values, predicting a ^{77}Se chemical shift tensor with a skew of the opposite sign; however, the SO calculation achieves improved agreement in δ_{iso}, δ_{ii}, Ω and arrives at a positive κ indicating that spin–orbit relativistic corrections are necessary in providing an accurate description of the shielding environment for the central selenium in $Se[N(^iPr_2PSe)_2]_2$ (Table 3). The orientation of the selenium chemical shift tensor calculated at the SC level is clearly incorrect given that the calculated skew is of opposite sign to that obtained experimentally. The SO DFT calculation orients the ^{77}Se chemical shift tensor with the intermediate component almost in the $SeSe_4$ plane, while the square plane nearly bisects the δ_{11}−Se−δ_{33} angle. The origin of the change in κ arises primarily from a large spin–orbit shielding perpendicular to the $SeSe_4$ plane that results in the principal component perpendicular to this plane changing from the least shielded component in the scalar calculation, to the most shielded component in the SO calculation.

The solid-state ^{125}Te NMR spectrum of $Te[N(^iPr_2PSe)_2]_2$ at 4.7 T is given in Figure 11 along with its simulation. Similar to the ^{77}Se chemical shift tensor of the selenium(II)

(131) Dietzsch, W.; Olk, R.-M.; Hoyer, E.; Meiler, W.; Robien, W. *Magn. Reson. Chem.* **1988**, *26*, 653–657.

complex, the tellurium chemical shift tensor has a positive skew; however, it possesses a considerably larger span and is closer to being axially symmetric than was found for the Se(II) center. The isotropic ^{125}Te chemical shift, 645 ppm, is similar to the value of 797 ppm found from a solution ^{125}Te NMR study of $C_4H_8TeI[N(Ph_2PSe)_2]$,[42] considering the tellurium chemical shift range exceeds 7000 ppm.[132] The value of $^1J(^{125}Te,^{77}Se)_{iso}$, ± 1200 Hz, agrees well with the indirect one-bond tellurium-selenium coupling constants from the solid-state ^{77}Se NMR results above, Table 2. Analogous to the molecular orbital theory description of the shielding explaining the positive skew for the selenium chemical shift tensor in $Se[N(^iPr_2PSe)_2]_2$, Figure 10 illustrates the dominant magnetic-dipole allowed mixing of orbitals involved in determining the tellurium chemical shift tensor. Similar to the calculations for the Se(II) complex, the calculated tellurium chemical shift tensor at the SC level of theory achieves poor agreement with the values of δ_{ii}, and a negative skew, while the SO calculation provides closer agreement to the experimental ^{125}Te chemical shift tensor and a positive skew. The SO calculation orients the ^{125}Te chemical shift tensor such that δ_{33} lies nearly perpendicular to the $TeSe_4$ plane, with δ_{22} within and δ_{11} slightly out of the square plane itself. The change in κ is, again, due primarily to a large spin–orbit shielding perpendicular to the $TeSe_4$ plane that essentially makes δ_{11}(SC), δ_{33} in the SO calculation. This shielding is, not surprisingly, larger than that found for the central selenium in the $Se[N(^iPr_2PSe)_2]_2$, which results in a tellurium chemical shift tensor with a larger positive skew; see Table 3.

Summary

Solid-state ^{31}P, ^{77}Se, ^{125}Te, and ^{195}Pt NMR spectroscopy was found to be a powerful comparative technique for the investigation of square-planar complexes of Group 10 (Pd^{II}, Pt^{II}) and 16 (Se^{II}, Te^{II}) centers coordinated with the tetraisopropyldiselenoimidodiphosphinate anion, $[N(^iPr_2PSe)_2]^-$. Density functional theory calculations support many of the experimentally observed trends and values in the chemical shift tensors, as well as provide orientations for the ^{14}N EFG tensors. Residual dipolar coupling effects between phosphorus and nitrogen were manifested in the ^{31}P MAS spectra for the selenium and tellurium complexes, but not for the palladium and platinum complexes. Very different orientations for the ^{14}N EFG tensors between the transition metal and main-group square-planar complexes account for the differences observed in solid-state ^{31}P NMR spectra at 4.7 and 7.0 T. Differences between the group 10 and 16 complexes were also found in the ^{77}Se MAS spectra of the diselenoimidodiphosphinato selenium environments, where considerably more variation is observed in the isotropic selenium chemical shifts of the Se(II) and Te(II) complexes than is found for those of Pd(II) and Pt(II). Additionally, characteristic spans and orientations for the selenium chemical shift tensors were found to differentiate diselenoimidodiphosphinato selenium environments within pseudoboat versus distorted-chair MSe_2P_2N heterocycles. The solid-state ^{77}Se, ^{125}Te, and ^{195}Pt NMR spectra for the central atom of the square-planar complexes investigated were found to have chemical shift tensors with positive skew values for the main-group square-planar complexes and a negative κ in the platinum complex. The different skews of the chemical shift tensors for the central atoms were rationalized with qualitative molecular orbital theory.

Acknowledgment. We thank the Natural Sciences and Engineering Research Council of Canada, the Alberta Ingenuity Fund, and the University of Alberta for research grants and scholarships. R.E.W. is a Canada Research Chair in Physical Chemistry at the University of Alberta. We thank Prof. Martin Cowie and his research group for access to their solvent stills and Dr. Devin Sears for use of his computational resources. Finally, we thank three anonymous reviewers for valuable comments.

Supporting Information Available: The calculated shielding tensors for the complexes investigated have been tabulated. This material is available free of charge via the Internet at http://pubs.acs.org.

IC7019999

(132) Luthra, N. P.; Odom, J. D. In *The Chemistry of Organic Selenium and Tellurium Compounds*; Patai, S., Rappoport, Z., Eds.; John Wiley & Sons: New York, 1986; Vol. *1*, pp 189–241..

(133) Jameson, C. J. In *Multinuclear NMR*; Mason, J., Ed.; Plenum Pres: New York, 1987; pp 89–131..

(134) Jameson, C. J. In *Phosphorus-31 NMR Spectroscopy in Stereochemical Analysis. Organic Compounds and Metal Complexes*; Verkade, J. G., Quin, L. D., Eds.; VCH Publishers, Inc.: Deerfield Beach, 1987; Vol. *8*, pp 205–230..